Emergence of metallic states at 2D MoSSe/GaAs Janus interface: A DFT study

Arwa Albar[1] and S. Assa Aravindh*[2]

[1]Physics Department, Faculty of Science, University of Jeddah, P.O Box 80327, Jeddah 21589, Saudi Arabia
[2]Nano and molecular systems research unit, University of Oulu, Pentti Kaiteran katu 1, Oulu, 90570, Finland

December 20, 2022

Abstract

The stability and the electronic properties of two dimensional (2D) GaAs/MoSSe Janus interfaces were investigated using first principles density functional theory calculations. The effect of different atomic terminations on the interface stability, electronic properties and charge transfer at the interfaces were analyzed. Metallic states are formed at the stable MoSSe/GaAs interface owing to the synergistic effect of the presence of 2D occupied antibonding states in MoSSe and the band alignment at the interface. The non-symmetric structure of MoSSe Janus material turns out to play a key role to control the electronic properties of the stable Janus interface, which will be crucial deciding factor for practical applications.

Keywords: 2D Janus material, semiconductor, heterostructures, density functional theory, electronic structure

1 Introduction

Since the exfoliation of graphene from graphite in 2004 [1], the research interest in 2D materials have grown drastically due to the discovery of novel properties and emerging applications of 2D materials. However, the zero-band gap of graphene has limited its applications in electronic and photovoltaic devices. In contrast to graphene, most 2D transition-metal dichalcogenides (TMDs) are semiconductors [2]. Particularly, many TMDs undergo indirect-to-direct band gap transition when a structural transition occurs from multilayer to monolayer, subsequently allowing them for applications in optoelectronic devices [3, 4]. One

*Assa.Sasikaladevi@oulu.fi

of the well-studied TMDs is MoS_2 monolayer, which possess a band gap of 1.8 eV, combined with high room-temperature current on/off ratio and large electron mobility of about 200 cm^2 V^{-1} S^{-1} [5]. These fascinating properties of 2D TMDs continue to motivate researchers to explore new avenues of 2D materials.

Recently, MoSSe, a Janus monolayer of transition metal dichalcogenides was successfully synthesized by replacing S atoms with Se atoms at one of the surfaces [6, 7]. The possibility of engineering the electronic and optical properties of Janus MoSSe layers for nanoelectronic applications have been proposed based on DFT simulations [8]. The out-of-plane broken symmetry and the permanent induced vertical dipole can drive distinct unique quantum phenomena which are desirable for future electronic devices [9]. Van der Waals heterostructures between different 2D materials are found to be a promising approach to design devices with properties on demand [10]. For instance, theoretical calculations revealed interesting electronic and optical properties for PtS_2/MoS_2 [11], ZnSe/AlAs [12], MoS_2/GaN [13] 2D van der Waals heterostructures. Janus heterostructures are also predicted to be excellent candidates for heterogeneous photocatalysis owing to the possibility of tuning the morphology by creating different interfaces such as metal/semiconductor or semiconductor/semiconductor as well as the ease of introducing alloying or defects at the interfaces [14]. It has been found in a recent study that Janus heterostructre of MoSSe/ZnO possess an indirect band gap with semiconducting properties and enhanced segregation of photo-generated carriers [15]. It has also been shown that the metallicity of Janus heterostructures can be tuned by varying the surface functionalization, such as metallic to half-metallic or semiconducting [16]. Among different Janus heterostructures that are being investigated, MoSSe/GaN heterostructures are found to be very promising for optoelectronic applications owing to the possibility of tuning the bandgap by changing the interface terminations [17]. Nevertheless, in the recent years, the interest in Janus based heterostructure have increased tremendously due to the advantage of their structures and excellent optoelectronic properties. Such properties are arising out of the chemical characteristics, quantum confinement and the dominant spin-orbit coupling at lower thicknesses [18].

Van der Waals (vdW) heterostructures formed by 2D materials containing GaAs have recently attracted interest owing to their applications in photocatalysis. In this connection, GaAs is a promising semiconductor material and the charge transfer that can occur by aligning with another favorable semiconductor material can be utilized for changing charge carrier dynamics [19, 20]. GaAs has been used widely in photodetector and solar cells [21, 22]. Interestingly, the 2D GaAs monolayer is stable and has excellent mechanical properties which are promising for wearable electronics [23]. Recently, Tian et al. synthesized Graphene/GaAs photodetector and obtained enhanced responsivity of the device [24]. This enhancement was attributed to the high surface state density of GaAs which causes confinement of the photogenerated carriers at the interface. Such effect leads to carrier multiplication and lowers the interface Fermi level which enhances the responsivity of the device. Thus, in our investigation,

we have considered the interface between MoSSe and GaAs to render similar enhancements which can have applications in photodetector. Nevertheless, GaAs turns out to be a promising semiconductor with band gap tunability to match with other semiconductors. In this scenario, we investigate the electronic properties of 2D Janus MoSSe/GaAs heterostructure considering the possible terminations. The motivation to study a heterostructure made between the monolayer of MoSSe and the monolayer of GaAs is to gather insights into the design of optoelectronic devices with desirable electronic properties. The advantage of MoSSe as compared to MoS_2 structures is the broken symmetry which has been reported to drive unique phenomena at the interfaces [25].

2 Computational methods

In this work, we use first principles density functional theory calculations to investigate the electronic properties of MoSSe/GaAs 2D Van der Waals heterostructure. The choice of the materials are based on the fact that both these monolayers have hexagonal symmetry, which thus minimizes the lattice mismatch of the interface. This choice is very important to determine an energetically favorable interface configuration. The Vienna Ab initio Simulation Package (VASP) was used to carry out the simulations [26]. The exchange and correlation functionals were treated in the Perdew-Burke-Ernzerhof generalized gradient approximation. The van der Waals corrections included in the calculations were that of Tkatchenko-Scheffler method as implemented in the VASP version 5.3.3. onwards [27]. A converged kinetic energy cutoff of 650 eV was employed to describe the plane waves included in the basis set. A Gamma-centered $1 \times 1 \times 1$ k-mesh is used to evaluate the interface electronic properties. Gaussian smearing is used with a smearing width of 0.05 eV. The energy convergence threshold to achieve self consistency was set to 10^{-6} eV. All crystal structures were relaxed until the forces on atoms are less than 0.001 eV/Å.

The 2D Janus interfaces were built using supercell sizes of $4\times4\times1$ and $5\times5\times1$ for GaAs and MoSSe, respectively. This results in a small lattice mismatch of 0.04% indicating that the net effect of strain on the physical properties will be negligible. Since MoSSe has either S or Se termination, this provides two possible interface heterostructures MoSSe/GaAs and MoSeS/GaAs which are considered in this work. A vacuum of size 21 Å is added to both interfaces along the z-direction in order to avoid the interaction between the repeated interfaces images due to periodicity. The resulting structures are shown in Fig. 1.

3 Results and discussion

The optimized lattice constants of 2D GaAs unit cell were $a = b = 4.0534$ Å and that of the 2D MoSSe were $a = b = 3.2439$ Å, respectively. Furthermore, the electronic band structures of the unit cells were calculated and shown in

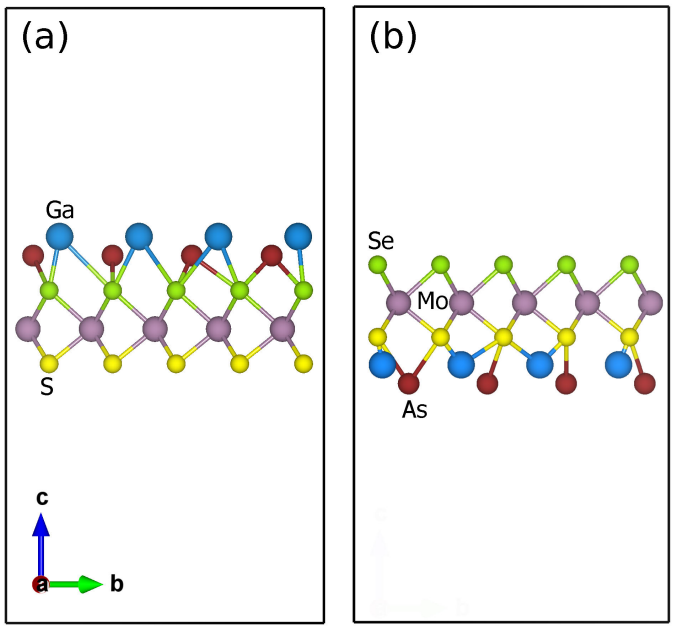

Figure 1: Optimized geometry of the MoSSe/GaAs interface structures. (a) Interface-Se and (b) Interface-S

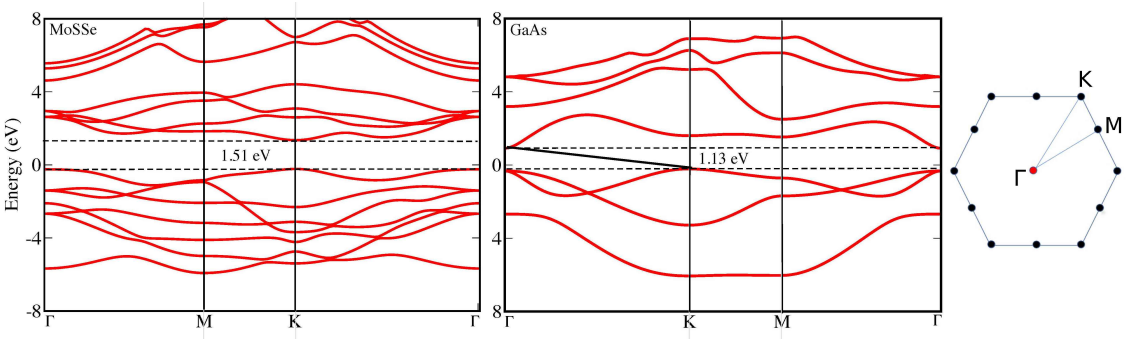

Figure 2: The band structure of the 2D unit cells of MoSSe and GaAs. he illustration at the right shows the Brillouin zone of hexagonal lattice.

Fig. 2. For the 2D GaAs, an indirect band gap of 1.13 eV was obtained whereas for 2D MoSSe a direct band gap of 1.51 eV was attained which is in line with previously reported values [28, 29].

After building the two possible interfaces, we have calculated the formation energies of the interfaces to find the most stable structure. The formation energies of the interfaces were calculated using the following equation [31]

$$E^f = E_{MoSSe/GaAs} - E_{GaAs} - E_{MoSSe} \tag{1}$$

Where $E_{MoSSe/GaAs}$ is the total energy of the interface structure, E_{GaAs} and E_{MoSSe} are the total energies of GaAs and MoSSe supercells. The formation energy for interface-Se (with Se atoms at the interface) was -4.21 eV while the formation energy for interface-S (with Sulfur atoms at the interface) was -38.36 eV. Since interface-S has much lower energy than interface-Se, this indicates that it is more favorable. In order to study the electronic properties of the interfaces, we have calculated the total and the local density of states of the two interfaces and shown in figure, Fig. 3. The results reveal the formation of metallic states at interface-S and an insulating character at interface-Se. The local density of states of interface-S in Fig. 3 (b) shows that the metallic states are due to Mo atoms. Moreover, the comparison in Fig. 4 shows that the Mo metallic states are due to localized *d*-orbitals. Hence, it is worthwhile to analyse the metallic states at interface-S as it is more energetically favorable structure. It is important to note that the negative formation energies obtained for the two interface terminations indicates that they both can be obtained experimentally (by controlling of growth conditions [30]), but one is more favorable. Since we have obtained entirely different electronic properties for the two interface terminations, as shown in Fig. 3 this demonstrates a new strategy to modify electronic properties by controlling the interface termination.

We perform charge density difference analysis for interface-S to explore the nature of metallicity at the interface and is shown in figure, Fig. 5. The results show the formation of extra electrons (blue) at As atoms and extra holes (yellow) at Mo atoms. Such observation indicates that a charge transfer occurs from MoSSe to GaAs across the interface. In order to determine the charge transfer driving force, we calculated the crystal orbital Hamilton population (COHP) [32] for GaAs, MoS and MoSe bonding, as shown in Fig. 6. For GaAs, unoccupied antibonding states are obtained slightly above the Fermi energy. On the other hand, MoS and MoSe bonding have occupied antibonding states just below the Fermi energy, which are energetically not stable. This observation implies that a charge transfer from MoSSe to GaAs is energetically favorable, in agreement with the differential charge density plot in Fig. 5.

Previously, graphene/GaAs interface was synthesized and revealed that defects in the GaAs can lead to significant change in properties. It is found that defects can tune band bending and thus reverse charge transfer direction; the lifetime of the excited electrons lowered by 6 times allowing ultrafast carrier dynamics [33]. On the other hand, applying the strain to 2D vdW heterostructure has been found to lower the band gap and forces indirect to direct band gap

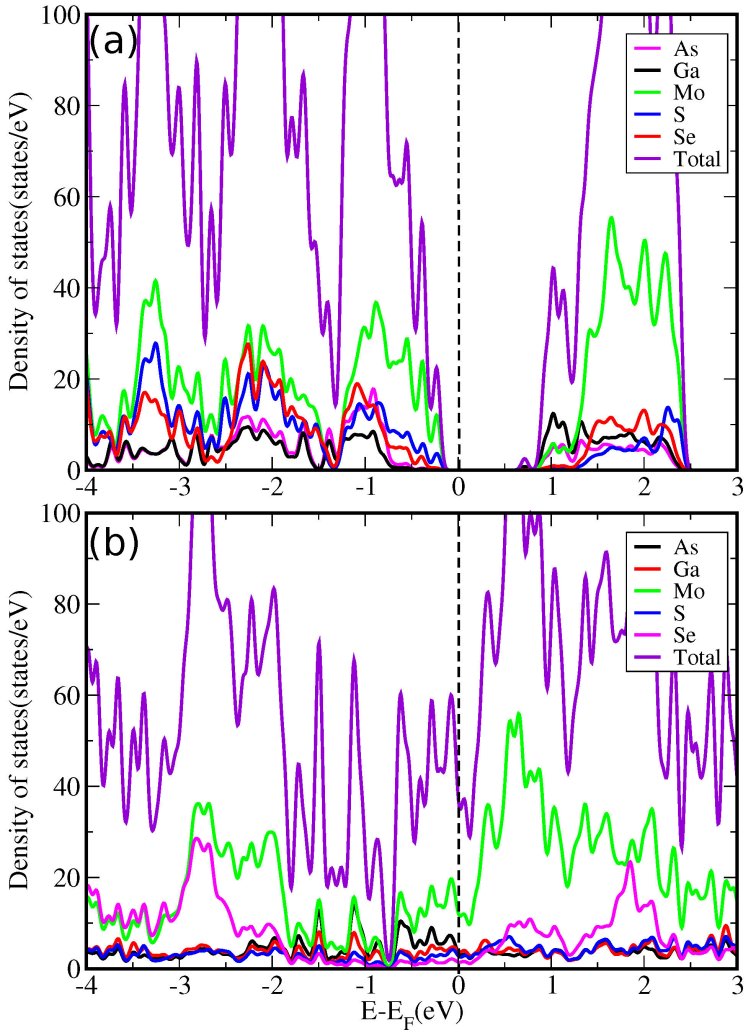

Figure 3: Local density of states for (a) Interface-Se and (b) Interface-S as specified in Figure 1.

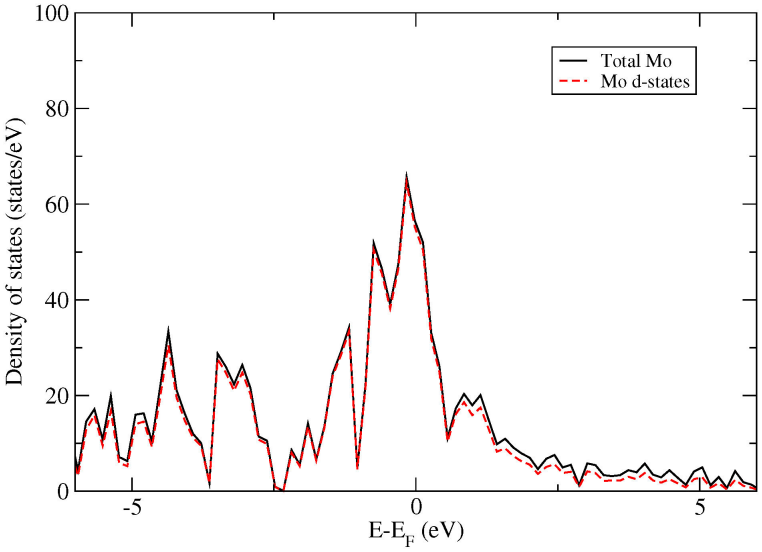

Figure 4: Total density of states of Mo atoms and the partial density of states of Mo d-orbitals for Interface-S

transition. Furthermore, the presence of suitable strain has been found to enhance carrier mobility and thus improve the efficiency of optoelectronic devices [34, 35]. Hence we presume that the charge redistribution at the interface can be significantly altered by the introduction of defects such as impurity atoms, or vacancies that can result in changes in optoelectronic properties.

To further analyze the origin of charge transfer, we calculated the band alignment for MoSSe/GaAs interface with S termination. The valence band offset (VBO) is calculated using [36]

$$VBO = (E_{MoSSe} + V_{MoSSe}) - (E_{GaAs} + V_{MoSSe}) + \Delta V \tag{2}$$

Where $E_{MoSSe} = -3.05$ eV and $E_{GaAs} = -4.19$ eV are the valence band maximum of bulk MoSSe and bulk GaAs. We obtained $V_{MoSSe} = -6.66$ eV and $V_{GaAs} = -3.80$ eV, which are the macroscopic average electrostatic potentials for the bulk materials. $\Delta V = 0.52$ eV is the shift of the averaged electrostatic potential energies across the interface. The obtained valence band offset is -1.20 eV. The conduction band edge is given by adding the band gap energy to the plotted valence band edge. Fig. 7 shows a band alignment of type II (staggered gap) for interface-S. The band alignment supports a charge transfer from MoSSe to GaAs which agree with our COHP results and explains the formation of metallic states at interface-S. Even though a large number of experimental works are still lacking in these kind of systems, the theoretical results obtained here can guide the design of optoelectronic devices with desirable electronic properties.

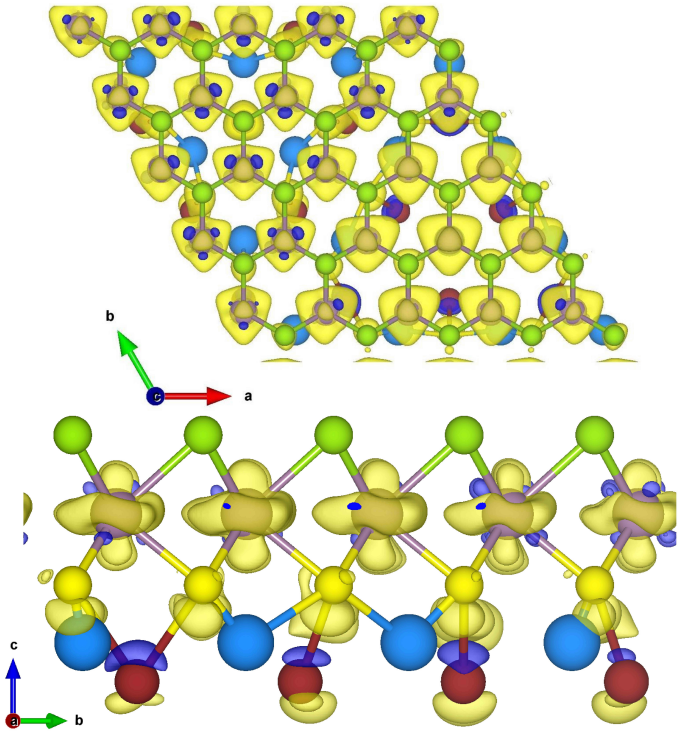

Figure 5: Top and side view of partial charge density difference plot for interface 2 of MoSSe/GaAs structure as specified in Figure 1. The bands are within an energy range -1 to 0 eV (with a value of 0.01 e/Å^3). Blue and yellow indicates electrons and holes, respectively.

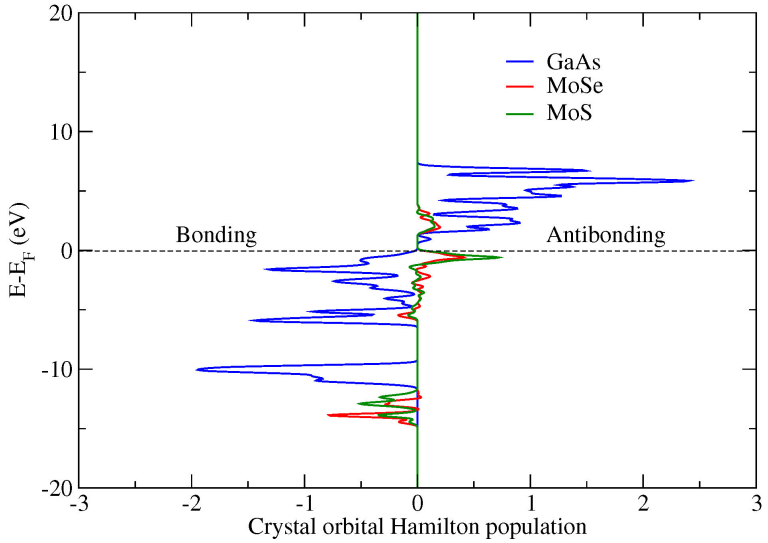

Figure 6: Crystal orbital Hamilton population for GaAs and MoSSe monolayers

.

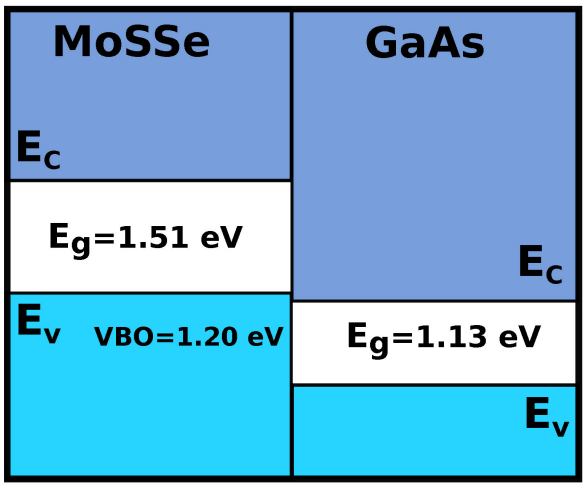

Figure 7: Band alignment diagram for interface-S of MoSSe/GaAs structure as specified in Figure 1

4 Conclusion

A density functional theory study was undertaken to provide theoretical understanding of the electronic properties at 2D Janus GaAs/MoSSe interface. Our investigation revealed the importance of interface atomic termination on the electronic and the structural properties of 2D Janus interfaces. Metallic states were obtained only at the interface with MoS termination while the interface with MoSe termination is insulating and energetically not favorable. Occupied antibonding states were found in MoSSe which drives the charge transfer from MoSSe to GaAs. The calculated band alignment demonstrated the presence of charge transfer from MoSSe to GaAs. Thus, the metallic states at GaAs/MoSSe interface can be attributed to the joint effect of the COHP and the band alignment. Therefore our results indicate that the stability and electronic properties of 2D Janus interfaces are affected by the interface termination which is critical for practical applications.

Declaration of competing interests The authors declare that they have no known competing financial interests or personal relationships that could have appeared to influence the work reported in this paper.

Acknowledgements This work was supported by the Academy of Finland (Grant No. 311934). The computing resources in this work are provided by CSC-IT Center for Science, Finland.

References

[1] Novoselov K S, Geim A K, Morozov S V, Jiang D, Zhang Y, Dubonos S V, Grigorieva I V and Firsov A A 2004 Electric Field Effect in Atomically Thin Carbon Films, *Science* 306 666-669.

[2] Choi W, Choudhary N, Han G H, Park J, Akinwande D and Lee Y H 2017 Recent Development of Two-Dimensional Transition Metal Dichalcogenides and their Applications *Mater. Today* 20 116-130.

[3] Ellis J K, Lucero M J and Scuseria G E 2011 The Indirect to Direct Band gap Transition in Multilayered MoS_2 as Predicted by Screened Hybrid Density Functional Theory *Appl. Phys. Lett.* 99 261908.

[4] Sun Y, Wang D and Shuai Z 2016 Indirect-to-Direct Band Gap Crossover in Few-Layer Transition Metal Dichalcogenides: A Theoretical Prediction *J. Phys. Chem. C* 120 21866-21870.

[5] Radisavljevic B, Radenovic A, Brivio J, Giacometti V and Kis A 2011 Single-Layer MoS_2 Transistors *Nat. Nanotechnol.* 6 147-150.

[6] Zhang J, Jia S, Kholmanov I, Dong L, Er D, Chen W, Guo H, Jin Z, Shenoy V B, Shi L and Lou J 2017 Janus Monolayer Transition-Metal Dichalcogenides *ACS Nano* 11 8192–8198.

[7] Lu A-Y, Zhu H, Xiao J, Chuu C-P, Han Y, Chiu M-H, Cheng C-C, Yang C-W, Wei K-H, Yang Y, Wang Y, Sokaras D, Nordlund D, Yang P, Muller D A, Chou M-Y, Zhang X and Li L-J 2017 Janus Monolayers of Transition Metal Dichalcogenides *Nat. Nanotechnol* 12 744-749.

[8] Barakat F, Laref A, Alsalhi M S and Farahi S 2020 The Impact of Anion Elements on the Engineering of the Electronic and Optical Characteristics of the Two Dimensional Monolayer Janus MoSSe for Nanoelectronic Device Applications *Results Phys.* 18 103284.

[9] Yagmurcukardes M, Qin Y, Ozen S, Sayyad M, Peeters F M, Tongay S and Sahin H 2020 Quantum Properties and Applications of 2D Janus Crystals and their Superlattices *Appl. Phys. Rev.* 7 011311.

[10] Winkler C, Harivyasi S S and Zojer E 2018 Controlling the Electronic Properties of Van der Waals Heterostructures by Applying Electrostatic Design *2D Mater.* 5 035019.

[11] Almayyali A O M, Kadhim B B and Jappor H R 2020 Tunable Electronic and Optical Properties of 2D PtS_2/MoS_2 Van der Waals Heterostructure *Physica E Low Dimens. Syst. Nanostruct.* 118 113866.

[12] Yao F, Zhou X and Xiong A 2020 Tunable Electronic and Optical properties of Two-Dimensional ZnSe/AlAs Van der Waals Heterostructure *Appl. Phys. A* 126 501.

[13] Gao R, Liu H, Liu H, Yang J, Yang F and Wang T 2020 Two-Dimensional MoS_2/GaN Van der Waals Heterostructures: Tunable Direct Band Alignments and Excitonic Optical Properties for Photovoltaic Applications *J. Phys. D: Appl. Phys.* 53 095107.

[14] Chauhan A, Rastogi M, Scheier P, Bowen C, Vasant Kumar R and Vaish R 2018 Janus Nanostructures for Heterogeneous Photocatalysis *Appl. Phys. Rev.* 5 041111.

[15] Cui Z, Bai K, Ding Y, Wang X, Li E, Zheng J and Wang S 2020 Electronic and Optical Properties of Janus MoSSe and ZnO vdWs Heterostructures *Superlattice. Microst.* 140 106445.

[16] Akgenc B 2020 Intriguing of two-dimensional Janus Surface-Functionalized MXenes: An Ab Initio Calculation *Comp. Mater. Sci.* 171 109231.

[17] Xu D, Zhai B, Gao Q, Wang T, Li J and Xia C 2020 Interface-Controlled band Alignment Transition and Optical Properties of Janus MoSSe/GaN vdW Heterobilayers *J. Phys. D: Appl. Phys.* 53 055104.

[18] Zhang L, Yang Z, Gong T, Pan R, Wang H, Guo Z, Zhang H and Fu X 2020 Recent Advances in Emerging Janus Two-Dimensional Materials: from Fundamental Physics to Device Applications *J. Mater. Chem. A* 8 8813-8830.

[19] Han S, Li Y, Chai J and Wang Z 2020 Study of the GaAs/SiH Van der Waals Type-II Heterostructure: a High Efficiency Photocatalyst Promoted by a Built-in Electric Field *Phys. Chem. Chem. Phys.* 22 8565-8571.

[20] Xu Y H, Fan Z Q, Zhang Z H and Zhao T 2021 Electronic and Transport Properties of GaAs/InSe Van der Waals Heterostructure *Applied Surface Science* 547 149174.

[21] Leem J W, Yu J S, Jun D H, Heo J and Park W K 2014 Efficiency Improvement of III–V GaAs Solar Cells Using Biomimetic TiO_2 Subwavelength Structures with Wide-Angle and Broadband Antireflection Properties *Sol. Energy Mater Sol. Cells* 127 43–49.

[22] Xu Z J, Lin S S, Li X Q, Zhang S J, Wu Z Q, Xu W L, Lu Y H and Xu S 2016 Monolayer MoS_2/GaAs Heterostructure Self-Driven Photodetector with Extremely High Detectivity *Nano Energy* 23 89–96.

[23] García A G, Pérez W L, Julio J R, Peteers F M, Estrada V M and Hernández R G 2018 Structural, Mechanical and Electronic Properties of Two-Dimensional Structure of III-Arsenide (1 1 1) Binary Compounds: An Ab-Initio Study *Comp. Mater. Sci.* 144 285–293.

[24] Tian H, Hu A, Liu Q, He X and Gui X 2020 Interface-Induced High Responsivity in Hybrid Graphene/GaAs photodetector *Adv. Optical Mater.* 8 1901741.

[25] Söz Ç K, Trosien S and Biesalski M 2020 Janus Interface Materials: A Critical Review and Comparative Study *ACS Materials Lett.* 2 336-357.

[26] Kresse G and Joubert D 1999 From Ultrasoft Pseudopotentials to the Projector Augmented-Wave Method *Phys. Rev. B* 59 1758-1775.

[27] Tkatchenko A and Scheffler M 2009 Accurate Molecular Van Der Waals Interactions from Ground-State Electron Density and Free-Atom Reference Data *Phys. Rev. Lett.* 102, 073005.

[28] Dong L, Lou J and Shenoy V 2017 Large In-Plane and Vertical Piezoelectricity in Janus Transition Metal Dichalchogenides *ACS Nano* 11, 8242-8248.

[29] Rozahun I, Bahti T, He G, Ghupur Y, Ablat A and Mamat M 2018 GaAs monolayer: Excellent SHG Responses and Semi Metallic to Metallic Transition Modulated by Vacancy Effect *Appl. Surf. Sci.* 441, 401-407.

[30] Fukidome H, Abe S, Takahashi R, Imaizumi K, Inomata S, Handa H, Saito E, Enta Y, Yoshigoe A and Teraoka Y 2011 Controls over Structural and Electronic Properties of Epitaxial Graphene on Silicon Using Surface Termination of 3C-SiC(111)/Si *Appl. Phys. Express* 4 115104.

[31] Liu J and Hua E 2017 High Photocatalytic Activity of Heptazine-Based g-C_3N_4/SnS_2 Heterojunction and Its Origin: Insights from Hybrid DFT *J. Phys. Chem. C* 121 25827-25835.

[32] Deringer V L, Tchougreeff A L and Dronskowski R 2011 Crystal Orbital Hamilton Population (COHP) Analysis As Projected from Plane-Wave Basis Sets *J. Phys. Chem. A* 115 5461-5466.

[33] Yang J, Sun Q, Liu W, Zhang Z, Hu X, Liu K, Yang H, Misawa H and Gong Q 2019 Engineering Ultrafast Carrier Dynamics at the Graphene/ GaAs Interface by Bulk Doping Level *Adv. Optical Mater.* 7 1900580.

[34] Guo W, Ge X, Sun S, Xie Y and Ye X 2020 The Strain Effect on the Electronic Properties of the MoSSe/WSSe vdW Heterostructure: a First-Principles Study *Phys. Chem. Chem. Phys.* 22 4946-4956.

[35] Yang S, Chen Y and Jiang C 2021 Strain Engineering of Two-Dimensional Materials: Methods, Properties, and Applications *InfoMat.* 3 397-420.

[36] Chen X, Guo G, Hao Y, Li J, Li W, Deng J, Zhang G and Zhai M 2020 First-Principles Investigation of Band Offset and Charge Transfer Characteristics at the PE/Fluorinated Layer Interface *Phys. Chem. Chem. Phys.* 22 22207-22216.